表面失效及防护

Adsorption of Amino Acid Inhibitors on Iron Surface: A First-principles Investigation

GUO Lei[1], *SHEN Xun*[1], *KAYA Savas*[2], *SHI Wei*[1], *ZHU Yan-li*[3]

(1.School of Material and Chemical Engineering, Tongren University, Tongren 554300, China;
2.Cumhuriyet University, Faculty of Science, Department of Chemistry, Sivas 58140, Turkey;
3.Sichuan Provincial Key Laboratory of Material Corrosion and Protection, Zigong 643000, China)

ABSTRACT: Amino acids are environment friendly organic inhibitors for most metals. The study on adsorption behavior of inhibitor molecules on metal surfaces has profound theoretical significance in understanding the anticorrosive mechanism and designing novel corrosion inhibitors. Based on first principles approach, the adsorption behaviour of three amino acid molecules (*i.e.*, glycine, alanine, and leucine) on iron surface was studied in linear combination of atomic orbitals method with the Dmol3 package. Firstly, the morphology parameters of iron crystal surface were calculated, and then a suitable crystal face was chosen as the adsorption surface. Finally, some parameters including adsorption energy and projected density of states were calculated to explain the inhibition mechanism. The Fe(110) surface was an optimal simulation surface among the three common faces. Three molecules exhibited vertical adsorption structure on Fe(110) surface. The absolute values of adsorption energy were 2.233 eV, 2.254 eV, and 2.472 eV for glycine, alanine and leucine, respectively. The results were consistent with rank of experimental inhibition efficiency. The adsorption can reduce work function value of Fe(110) substrate. The Hirshfeld charge analysis shows that there is an electronic transfer process from the inhibitors to Fe substrate in all chemisorbed configurations. The analysis of state density suggests that several covalent bonds are formed between active atoms and Fe surface atoms in amino acid molecules. Bond energy plays a decisive role in the inhibitive efficiency of corresponding inhibitors.

KEY WORDS: carbon steel; corrosion inhibitor; amino acid; adsorption; first-principles; Dmol[3]
中图分类号：TG174.42 **文献标识码：**A **文章编号：**1001-3660(2017)04-0228-07
DOI：10.16490/j.cnki.issn.1001-3660.2017.04.037

几种氨基酸类缓蚀剂在铁表面吸附的第一性原理研究

郭雷[1]，沈珣[1]，KAYA Savas[2]，石维[1]，朱艳丽[3]

（1.铜仁学院 材料与化学工程学院，贵州 铜仁 554300;
2.土耳其共和国大学 理学院化学系，土耳其 锡瓦斯 58140；
3.材料腐蚀与防护四川省重点实验室，四川 自贡 643000）

Received：2016-12-29；**Revised**：2017-01-09
收稿日期：2016-12-29；**修订日期**：2017-01-09
Fund：Supported by the National Natural Science Foundation of China (51462030), the Science and Technology Program of Guizhou Province (QKHJC2016-1149), the Research Fund for the Doctoral Program of Tongren University (trxyDH1510), Guizhou Provincial Department of Education Foundation (QJHKYZ2016-105), the Opening Project of Sichuan University of Science and Engineering (2016CL06), and the student's platform for innovation and entrepreneurship training program (2016106665)
基金项目：国家自然科学基金（51462030）；贵州省科学技术基金（QKHJC2016-1149）；铜仁学院博士科研启动基金（trxyDH1510）；贵州省普通高等学校科技拔尖人才支持计划（QJHKYZ2016-105）；材料腐蚀与防护四川省重点实验室开放基金（2016CL06）；国家级大学生创新创业训练计划（2016106665）

Biography：GUO Lei (1987—), Male, Doctor, Associate professor, Research focus: corrosion and protection of metal materials.
作者简介：郭雷（1987—），男，博士，副教授，主要研究方向为金属材料的腐蚀与防护。

摘　要：目的 氨基酸是一类重要的环境友好型金属有机缓蚀剂，研究缓蚀剂分子在金属表面的吸附行为，对深入理解缓蚀机理及设计新型缓蚀剂分子有重要的理论意义。**方法** 基于第一性原理框架下的原子轨道线性组合方法，采用 Dmol^3 软件研究了甘氨酸、丙氨酸和亮氨酸三种分子在铁表面的吸附行为。首先对铁晶体表面的形貌学参数进行了计算，然后选取合适的晶面作为吸附表面。最后通过计算三种分子在铁表面的吸附能和分波态密度等参数分析缓蚀机制。**结果** 铁的三种常见晶面中，Fe(110)面为最佳吸附表面。三种氨基酸分子在 Fe(110)表面呈竖直型吸附构型，甘氨酸、丙氨酸和亮氨酸的吸附能绝对值大小分别为 2.233、2.254、2.472 eV，这与其实验缓蚀效率大小顺序相一致。**结论** 缓蚀剂分子吸附可导致金属基底的功函数减小。Hirshfeld 电荷分析表明，吸附过程中存在从氨基酸分子到 Fe(110)表面的电子转移现象。态密度分析表明，氨基酸分子中的活性原子与铁表面原子形成了共价键，键能的大小对缓蚀剂分子的缓蚀效率起决定性作用。

关键词：碳钢；缓蚀剂；氨基酸；吸附；第一性原理；Dmol^3

The corrosion of metal can result in a great economic loss for the industry, and one of the most efficient methods to protect metals is the use of organic inhibitors[1—3]. We usually think that the inhibitors can be adsorbed on the metallic surfaces, which can slow down the cathodic reduction reaction and the anodic dissolution process of the metals[4—5]. In fact, the anticorrosive mechanism in the aqueous phase is very complex, and it can be viewed as a result of several competing effects as described below.

As shown in Fig.1, there is usually four different interaction forms in a realistic corrosive environment, *i.e.*, the interplay between the inhibitor-solvent, substrate-solvent, inhibitor-substrate, and solvent-solvent interactions. Generally, most researchers suggest that the inhibitor-substrate interaction plays a decisive and leading role in the adsorption process because there usually exist strong chemical bonds between them[6—8]. The solvent (usually water molecule) interacts weakly with the hydrophobic substrate such as iron and therefore can be easily replaced by inhibitors. Under this circumstance, the substrate/vacuum model appears reasonable to research the adsorption behaviour of corrosion inhibitors on the metal surface. Among the organic inhibitors, amino acid compounds are attractive owing to their nontoxicity, biodegradability and cost efficiency. However, little attention has been paid to how these organic surface modifiers bind to metal surfaces, and why seemingly minor modifications in the structures of organic active compounds can have a profound effect on their inhibition efficiency. Many researchers[9—12] have investigated the interactions between organic inhibitors and metal surface by molecular dynamics simulation method, in gas phase or aqueous phase. However, one can only perform qualitative analysis by this approach, and it is very embarrassing for force field to describe the electron transfer processes. On the other hand, density functional theory (DFT) stands out from all first-principles quantum mechanical methods for the simulation of materials, as it enables very good approximations for the complicated components of electronic motion called exchange and correlation[13—15]. It is helpful to develop novel corrosion inhibitor molecules in an efficient and cost-effective manner for use in a number of corrosion systems for domestic and industrial applications[16].

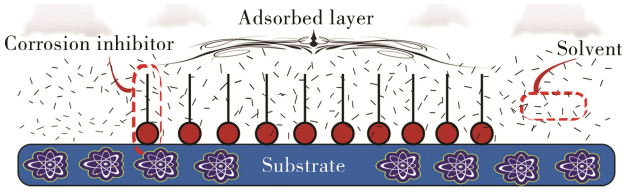

Fig.1 Typical schematic of the anticorrosion mechanism for corrosion inhibitors

图 1　腐蚀抑制剂防腐蚀机理的典型示意图

In this work, we focused on the adsorption of glycine, alanine, and leucine on the surface of iron using DFT calculations. The studied amino acid molecules have proven experimentally to be efficient against the corrosion of steel in HCl solution, and the inhibition efficiency follows the order: glycine < alanine < leucine[17]. In order to study the micro-process of corrosion inhibition, the most stable adsorption configurations, work function changes, density of states, as well as charge density difference were theoretically analyzed.

1　Computational Methods and Modeling

Firstly, to select an appropriate adsorption surface, the crystal "Morphology" module within Materials Studio (MS, BIOVIA Inc.) was used to predict the morphological characteristic of the iron facets. Then, all other DFT calculations in this work were performed using the DMol^3 module[18] (also embedded in MS) with numerical atomic orbital basis sets. The exchange-correlation functional of Perdew, Burke, and Ernzerh of (PBE)[19] was adopted. The double-numerical plus polarisation (DNP) basis sets were used in the expansion of the Kohn-Sham orbitals and the orbital confining cut-off was set as 0.46 nm. A Fermi smearing of 0.001 Ha was also used to improve computational performance. The core electrons of all of the atoms were represented by DFT semi-core pseudopotentials (DSPP)[20], where the effect of core electrons is substituted by a simple potential including some degree of relativistic effects. A 6×6×1 Monkhorst- Pack *k*-point mesh was utilized to sample the Brillouin zone of the unit cell. Spin polarization was used when needed.

All calculations used slabs of four layers with the bottom two layers constrained in their bulk positions

and the top two layers along with the adsorbate were allowed to fully relax. A vacuum thickness of 2 nm was used to separate each slab from its neighbouring images along the *z*-direction. For the geometry optimization calculations, the convergence tolerance was set to 1×10^{-6} Ha for energy, 0.02 Ha/nm for maximum force, and 0.0005 nm for maximum displacement. Moreover, the self-consistent field (SCF) tolerance was set to 1×10^{-6} Ha with multipolar expansion through an octupole moment. For further computational details see our previous publications, in particular Ref. [21] and also Ref.[22]. The calculated lattice constant of α-iron is 0.288 nm, which is in good agreement with the relevant literature[23—24].

Generally, the hydrogen atom in carboxy group can be easily cut down on metal surfaces[25], but the dissociated hydrogen atom does not significantly perturb the deprotonated molecule adsorbed on Fe(110). Therefore, we only consider deprotonated amino acids to be discussed. The initial adsorption modes were shown in Fig. 2. The adsorption energy, E_{ads}, was defined as:

$$E_{ads} = E_{H_2NCHRCOO(ads)} + E_{H(ads)} - (E_{H_2NCHRCOOH(g)} + 2E_{Fe(s)}) \quad (1)$$

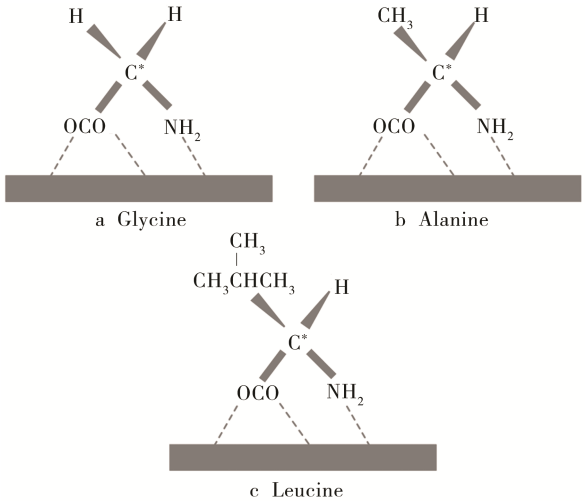

Fig.2 Schematic representations of glycine (a), alanine (b), and leucine (c) bound to a metal surface

图 2 甘氨酸、丙氨酸和亮氨酸与金属表面结合的示意图

Where $E_{H_2NCHRCOO(ads)}$ is the total energy of the system containing the adsorbed deprotonated amino acid, $E_{H(ads)}$ is the total energy of the system containing the adsorbed single hydrogen, $E_{H_2NCHRCOOH(g)}$ is the total energy for the amino acid in the gas phase, $E_{Fe(s)}$ is the total energy for the optimized solid Fe surface. By this definition, a negative value is favorable to the adsorption.

2 Results and Discussions

2.1 An Investigation of Iron Surfaces

The "Morphology" module provides three different methods of calculating the habit of a crystal from its internal crystal structure: Bravais-Friedel Donnay-Harker (BFDH) method, growth morphology (GM) algorithm, and equilibrium morphology (EM) method. More details about these methods are given in References [26—27]. The calculated morphology parameters for iron crystal through the three algorithms are summarized in Table 1. It can be seen that the (110) face possesses the largest proportion of the total crystal surface area. As shown in Fig.3, for the three typical kinds of iron surfaces, Fe(111) and Fe(100) surfaces have relatively open structures, while Fe(110) is a density packed surface and has the most stabilization, and it has large enough surface area to contact with the adsorbate, so we choose Fe(110) surface for the subsequent simulation calculations.

Tab.1 Calculated morphology parameters for iron crystal through different algorithms

表 1 不同算法下铁晶体的形态参数

hkl	Total facet area/nm^2			Total facet area/%		
	EM	GM	BFDH	EM	GM	BFDH
(110)	7.98×10^6	4.16×10^3	4.13×10^2	63.31	83.39	100
(100)	3.07×10^6	5.47×10^2		24.38	11.61	
(111)	1.55×10^6			12.29		

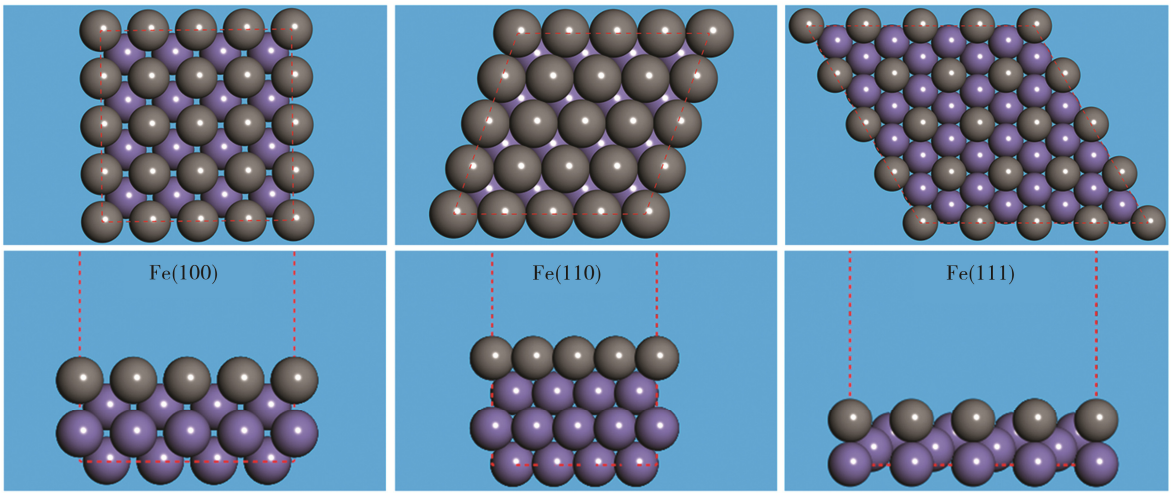

Fig.3 Top and side views of the Fe(100), Fe(111), and Fe(110) surfaces (Balls in gray color denote the atoms at the first surface layer)

图 3 Fe(100)、Fe(111)和 Fe(110)面的顶视图和侧视图（灰色球表示最外层原子）

2.2 Adsorption Geometries and Energies

The most stable configurations for the dissociative adsorption of glycine, alanine, and leucine on Fe(110) surface are displayed in Fig.4. Some structural information as well as experimental corrosion rate and inhibition efficiency are summarized in Table 2. As expected, the deprotonated molecule exhibits tridentate bonding with the iron atoms through the nitrogen atom and two oxygen atoms. Based on the data in Table 1, the N—Fe and O—Fe bond lengths are in the range between 0.2~0.22 nm, which is comparable to the sum of N/O and Fe atomic covalent radii ($r_{cov}^{N} + r_{cov}^{Fe}$ =0.071+0.132=0.203 nm, $r_{cov}^{O} + r_{cov}^{Fe}$ = 0.066+0.132=0.198 nm)[28]. This implies that the chemisorption really exists between three inhibitors and the iron surface.

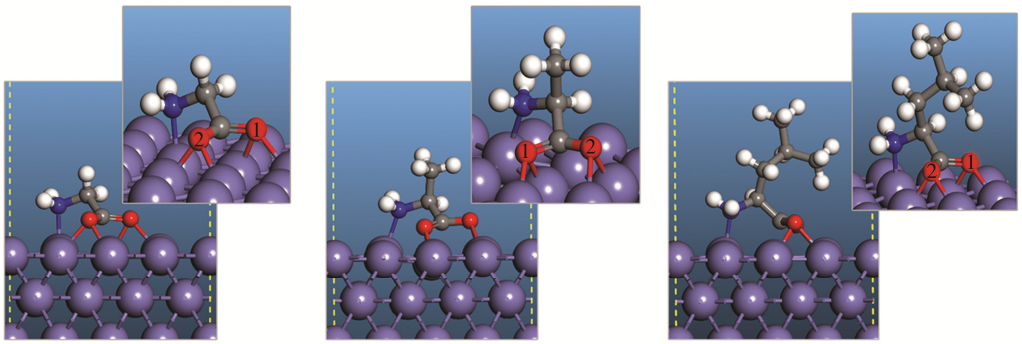

a Glycine　　b Alanine　　c Leucine

Fig.4 Top and side views of the most stable configurations for the dissociative adsorption of glycine (a), alanine (b), and leucine (c) on Fe(110) surface (Only parts of the atoms of the slab model are shown for clarity)

图 4　甘氨酸、丙氨酸和亮氨酸在 Fe(110)晶面上离解吸附最稳定构型的顶视图和侧视图（为了清晰起见，仅显示了平板模型的部分原子）

The adsorption energies for glycine, alanine, and leucine on Fe(110) surface are −2.233 eV, −2.254 eV, and −2.472 eV, respectively. Thus, leucine gives the highest interaction energy of the three inhibitors, which can be attributed to its slightly longer carbon chains in the hydrophobic part. Many reports show that alkyl chain length plays an important role in the inhibition efficiency (IE)[29—30]. The IE values of inhibitors evaluated can first increase and then decrease with the length of the alkyl chain, this changes can be explained as a result of the flexibility of alkyl chain. Because of the strong chemisorption, the adsorption-induced corrugation, as measured by Δh_{Cu} (defined in Table 2), is about 0.014~0.018 nm. This phenomenon also occurs in our previous work[31] about the adsorption of triazole derivatives on the copper surface.

Tab.2 Calculated parameters for inhibitors on the Fe(110) surface: minimum N/O-Fe distance ($d_{N,Fe}$, $d_{O,Fe}$) maximum vertical displacement of the surface Fe in contact with the inhibitor (Δh_{Fe}), adsorption energies (E_{ads}), and the experimentally evaluated corrosion rate (v) and inhibition efficiency (IE)

表 2　Fe(110)晶面上抑制剂的计算参数

Compd.	$d_{N,Fe}$/nm	$d_{O1,Fe}$/nm	$d_{O2,Fe}$/nm	Δh_{Fe}/nm	E_{ads}/eV	v[a]/(mm·a^{-1})	IE[a]/%
Glycine	0.2177	0.2044	0.2045	0.0145	−2.233	3.33	78.9
Alanine	0.2249	0.2031	0.2039	0.0176	−2.254	3.13	80.2
Leucine	0.2165	0.2023	0.2006	0.0179	−2.472	1.31	90.6

[a] Reference [17].

2.3 Adsorption Induced Work Function Changes

The surface electron work function (EWF) is one of the most fundamental properties of a metallic surface. It is the minimum energy required to remove an electron from a solid to a point immediately outside the solid surface. A practical way of evaluating work function is to compare the values of the Fermi energy (E_F) and that of the electrostatic potential in a vacuum (V_e) away from the surface, *i.e.*, EWF=V_e–E_F[32]. In this work, the average potential profiles along z axis for clean and modified Fe(110) surfaces are shown in Fig.5. The obtained EWF values for clean, glycine-, alanine-, and leucine- modified Fe(110) surfaces are 0.159 Ha, 0.147 Ha, 0.146 Ha, and 0.149 Ha, respectively. This behavior of the work function variation is similar to that calculated theoretically for the adsorption of the benzotriazole on reduced and oxidized copper surfaces[33]. Then

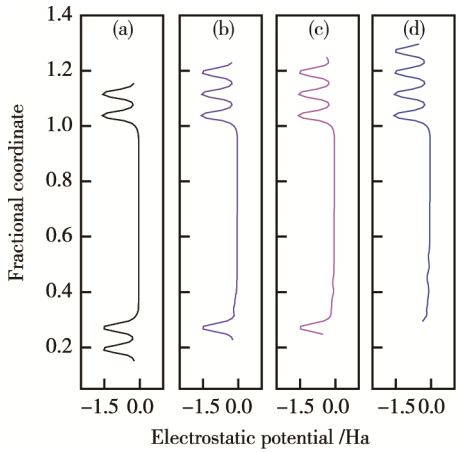

Fig.5 The average potential profiles along z axis for clean (a), glycine- (b), alanine- (c), and leucine- (d) modified Fe(110) surfaces

图 5　z 轴平均电位分布

we can conclude that the reduced work function after adsorption should diminish any reaction that donates electron(s) to the metal, such as the adsorption of corrosive chloride anions ($Cl^-_{solv} \rightarrow Cl_{ads}+e_{metal}$), dissolution of metal (*e.g.*, $Fe_{solid} \rightarrow Fe^{2+}_{solv}+2e_{metal}$), or oxidation of metal (*e.g.*, $2Fe+O_2+H_2O \rightarrow Fe_2O_3+2H^++2e$).

2.4 Projected Density of States

Analysis of the projected density of states (DOS) of the adsorption can give an indication of the inhibitor–substrate bonding interaction that occurs. As shown in Fig. 6, the DOS for iron atoms in the first substrate layer consists mainly of narrow 3*d*-band. Generally, the most relevant states for chemisorption are those located around the Fermi energy (E_F)[34]. While Fe has a large density of *d*-states at the E_F. Besides, the orbital of the different reactive sites (N and O atoms) in the inhibitors have the corresponding peak values at some same energy level with Fe 3*d*-orbitals. This indicates that a strong hybridization may occur between them. We also found that the DOS for the second layer Fe atoms show very little change after adsorption. This means that there is some interaction between this substrate atom and amino acid, but it is not as strong as with the surface Fe atoms.

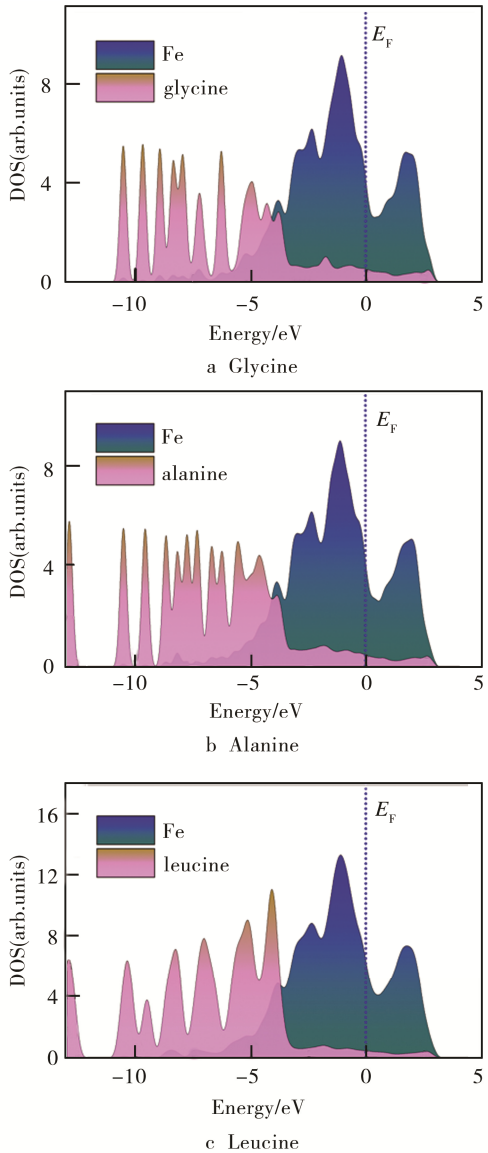

Fig.6 Density of states projected to inhibitors and Fe atoms for the three stable adsorption configurations in Fig.4

图 6 图 4 三种稳定吸附结构中抑制剂和 Fe 原子的状态密度

2.5 Charge Density Difference

To further understand the adsorption of amino acid molecules on Fe(110) surface, we calculate the charge density difference ($\Delta\rho$), which is defined as follows[31]:

$$\Delta\rho=\rho_{mol/sur}(r)-\rho_{sur}(r)-\rho_{mol}(r) \quad (2)$$

Where $\rho_{mol/sur}(r)$, $\rho_{sur}(r)$, and $\rho_{mol}(r)$ are the total density difference of the system, the clean surface of iron, and the isolated amino acid molecules, respectively. The electron density difference for the three adsorption configurations is shown in Fig.7. Blue and red regions indicate the electron accumulation and depletion, respectively. We can see that the electron density is depleted from amino acids molecules, and accumulates on the iron atoms (blue area), which indicates the forming of the covalent bonds. Hirshfeld charge analysis shows that the total charge of modified iron surface is negative, and the values are −0.14 e, −0.16 e and −0.18 e from glycine to alanine and leucine systems. This suggests that leucine has the strongest electron-donating ability and then presents the best corrosion inhibition performance, which is consistent with the experimental observations.

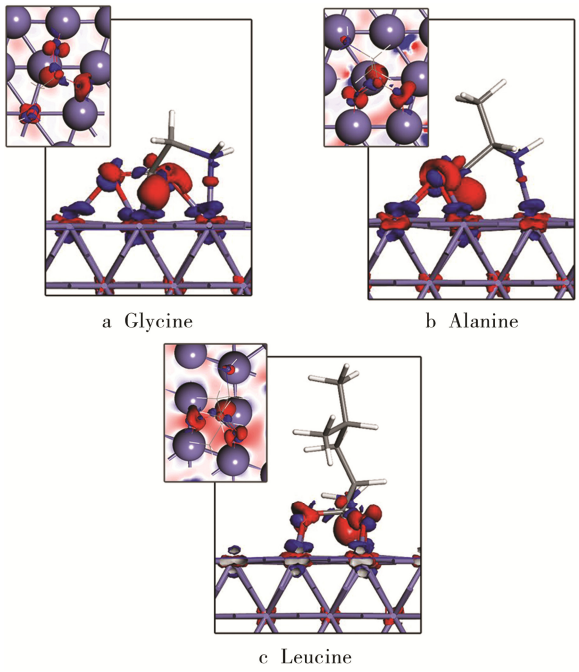

Fig.7 Charge density difference for the glycine-, alanine-, and leucine-modified Fe(110) systems (The blue region denotes electronic accumulation, while the red region represents electronic loss)

图 7 甘氨酸、丙氨酸和亮氨酸修饰的 Fe(110)体系的电荷密度差（蓝色区域表示电子积累，而红色区域表示电子损失）

3 Conclusions

The present work aims to understand the iron corrosion inhibition mechanism. We investigated in details the interaction of three amino acid molecules with the Fe(110) surface. Our intensive DFT calculations show that the dehydrogenated amino acid molecules have strong coupling with the Fe(110) surface. During the adsorption process, electrons were transferred from the amino acids molecules to the substrate. The plot of the DOS indicates that there exist covalent bonds between the inhibitor molecule and the surface atoms. The calculation results obtained and analyzed in this paper provided fundamental information which is difficult to obtain in experiments. The findings will contribute to the understanding of the anticorrosive mechanism of similar organic inhibitors.

References

[1] LI X G, ZHANG D W, LIU Z Y, et al. Share Corrosion Data[J]. Nature, 2015, 527 (7579): 441—442.

[2] RANI B E A, BASU B B J. Green Inhibitors for Corrosion Protection of Metals and Alloys: An Overview[J]. International Journal of Corrosion, 2012, 2012: 1—15.

[3] MIHAJLOVIC M B P, ANTONIJEVIC M M. Copper Corrosion Inhibitors: A Review[J]. International Journal of Electrochemical Science, 2015, 10(2): 1027—1053.

[4] FINŠGAR M, JACKSON J. Application of Corrosion Inhibitors for Steels in Acidic Media for the Oil and Gas Industry: A Review[J]. Corrosion Science, 2014, 86: 17— 41.

[5] RAJA P B, ISMAIL M, GHOREISHIAMIRI S, et al. Reviews on Corrosion Inhibitors: A Short View[J]. Chemical Engineering Communications, 2016, 203 (9): 1145—1156.

[6] KOKALJ A, PELJHAN S. Density Functional Theory Study of ATA, BTAH, and BTAOH as Copper Corrosion Inhibitors: Adsorption onto Cu(111) from Gas Phase[J]. Langmuir, 2010, 26 (18): 14582—14593.

[7] RADILLA J, NEGRON-SILVA G E, PALOMAR-PARDAVE M, et al. DFT Study of the Adsorption of the Corrosion Inhibitor 2-mercaptoimidazole onto Fe(100) Surface[J]. Electrochimica Acta, 2013, 112: 577—586.

[8] WANG D, GAO L, ZHANG D, et al. Experimental and Theoretical Investigation on Corrosion Inhibition of AA5052 Aluminium Alloy by L-cysteine in Alkaline Solution[J]. Materials Chemistry and Physics, 2016, 169: 142—151.

[9] OGUZIE E E, OGUZIE K L, AKALEZI C O, et al. Natural Products for Materials Protection: Corrosion and Microbial Growth Inhibition Using Capsicum Frutescens Biomass Extracts[J]. ACS Sustainable Chemistry & Engineering, 2013, 1 (2): 214—225.

[10] FU J J, LI S N, WANG Y, et al. Computational and Electrochemical Studies of Some Amino Acid Compounds as Corrosion Inhibitors for Mild Steel in Hydrochloric Acid Solution[J]. Journal of Materials Science, 2010, 45(22): 6255—6265.

[11] KHALED K F, AMIN M A. Corrosion Monitoring of Mild Steel in Sulphuric Acid Solutions in Presence of Some Thiazole Derivatives: Molecular Dynamics, Chemical and Electrochemical Studies[J]. Corrosion Science, 2009, 51(9): 1964—1975.

[12] KAYA S, GUO L, KAYA C, et al. Quantum Chemical and Molecular Dynamic Simulation Studies for the Prediction of Inhibition Efficiencies of Some Piperidine Derivatives on the Corrosion of Iron[J]. Journal of the Taiwan Institute of Chemical Engineers, 2016, 65: 522—529.

[13] SKYLARIS C K. Physics: A Benchmark for Materials Simulation[J]. Science, 2016, 351 (6280): 1394—1395.

[14] GEERLINGS P, DE PROFT F, LANGENAEKER W. Conceptual Density Functional Theory[J]. Chemical Reviews, 2003, 103 (5): 1793—1873.

[15] 廉兵杰, 石泽民, 徐慧, 等. 唑类缓蚀剂在铜表面的吸附机理[J]. 表面技术, 2015, 44 (12): 19—26.
LIAN Bing-jie, SHI Ze-min, XU hui, et al. Adsorption Mechanism of Azole Corrosion Inhibitors on Cu Surface[J]. Surface Technology, 2015, 44 (12): 19—26.

[16] GECE G. The Use of Quantum Chemical Methods in Corrosion Inhibitor Studies[J]. Corrosion Science, 2008, 50 (11): 2981—2992.

[17] ASHASSI-SORKHABI H, MAJIDI M R, SEYYEDI K. Investigation of Inhibition Effect of Some Amino Acids Against Steel Corrosion in HCl Solution[J]. Applied Surface Science, 2004, 225 (1—4): 176—185.

[18] DELLEY B. From Molecules to Solids with the DMol3 Approach[J]. Journal of Chemical Physics, 2000, 113 (18): 7756—7764.

[19] PERDEW J P, BURKE K, ERNZERHOF M. Generalized Gradient Approximation Made Simple[J]. Physical Review Letters, 1996, 77 (18): 3865—3868.

[20] DELLEY B. Hardness Conserving Semilocal Pseudopotentials [J]. Physical Review B, 2002, 66 (15): 155125.

[21] GUO L, ZHU S, LI W, et al. Electrochemical and Quantum Chemical Assessment of 2-aminothiazole as Inhibitor for Carton Steel in Sulfuric Acid Solution[J]. Asian Journal of Chemistry, 2015, 27 (8): 2917—2923.

[22] CHEN R X, GUO L, XU S Y. Experimental and Theoretical Investigation of 1-hydroxybenzotriazole as a Corrosion Inhibitor for Mild Steel in Sulfuric Acid Medium[J]. International Journal of Electrochemical Science, 2014, 9 (12): 6880—6895.

[23] ARYA A, CARTER E A. Structure, Bonding, and Adhesion at the TiC(100)/Fe(110) Interface from First Principles[J]. Journal of Chemical Physics, 2003, 118 (19): 8982—8996.

[24] LU M, CHIEN C L. Structural and Magnetic Properties of Fe-W Alloys[J]. Journal of Applied Physics, 1990, 67 (9): 5787—5789.

[25] NOBUHARA K, NAKANISHI H, KASAI H, et al. Interactions of Atomic Hydrogen with Cu(111), Pt(111), and

Pd(111)[J]. Journal of Applied Physics, 2000, 88 (11): 6897—6901.

[26] SCHMIDT C, ULRICH J. Predicting Crystal Morphology Grown From Solution[J]. Chemical Engineering & Technology, 2012, 35 (6): 1009—1012.

[27] ZHOU K, LI J, LUO J H, et al. Crystal Growth, Structure and Morphology of Rifapentine Methanol Solvate[J]. Chinese Journal of Chemical Engineering, 2012, 20 (3): 602—607.

[28] PYYKKO P, ATSUMI M. Molecular Single-bond Covalent Radii for Elements 1-118[J]. Chemistry-A European Journal, 2009, 15 (1): 186—197.

[29] PALOMAR-PARDAVE M, ROMERO-ROMO M, HERR--ERA-HERNANDEZ H, et al. Influence of the Alkyl Chain Length of 2-amino 5-alkyl 1,3,4-thiadiazole Compounds on the Corrosion Inhibition of Steel Immersed in Sulfuric Acid Solutions[J]. Corrosion Science, 2012, 54: 231—243.

[30] GONG Y, WANG Z, GAO F, et al. Synthesis of New Benzotriazole Derivatives Containing Carbon Chains as the Corrosion Inhibitors for Copper in Sodium Chloride Solution[J]. Industrial & Engineering Chemistry Research, 2015, 54 (49): 12242—12253.

[31] GUO L, DONG W P, ZHANG S T. Theoretical Challenges in Understanding the Inhibition Mechanism of Copper Corrosion in Acid Media in the Presence of Three Triazole Derivatives[J]. RSC advances, 2014, 4 (79): 41956—41967.

[32] MICHAELSON H B. Work Function of Elements and Its Periodicity[J]. Journal of Applied Physics, 1977, 48 (11): 4729—4733.

[33] KOKALJ A. Ab initio Modeling of the Bonding of Benzotriazole Corrosion Inhibitor to Reduced and Oxidized Copper Surfaces[J]. Faraday Discussions, 2015, 180: 415—438.

[34] KOVACEVIC N, KOKALJ A. Chemistry of the Interaction between Azole Type Corrosion Inhibitor Molecules and Metal Surfaces[J]. Materials Chemistry and Physics, 2012, 137 (1): 331—339.